Geant4 Analysis of Secondary Neutrons in Proton Therapy

Alice Roux, Steve Peterson and Tanya Hutton

Department of Physics, University of Cape Town, South Africa, 7700

E-mail: rxxali002@myuct.ac.za

Abstract. In proton therapy, secondary radioactive particles are produced along the beam line and within the patient due to proton interactions with nuclei in their path. Secondary neutrons are of particular concern, as they are hard to detect and have a high biological effectiveness which causes more damage than other particles to tissues. The Geant4 simulation toolkit was used to model the path of a 191 MeV proton beam through a copper collimator with an inner radius of 50mm, and into a water phantom, which mimics the 24cm proton beam at iThemba LABS. Most internal neutron production was found to occur before the Bragg peak once the proton energies have lowered and the cross section for neutron producing reactions is maximised. For a beam with radius 60mm, 40% of the neutron current comes from external sources. These external neutrons contributed 63% of the neutron associated dose whih comprised 95% of the total absorbed dose. The simulation is able to measure the neutron energy fluence through various planes corresponding to the placement of neutron detectors for future experiments. This shows where neutron production and attenuation occurs within a treatment scenario.

1. Introduction

When compared to traditional radiotherapy, proton therapy delivers more precise positioning of the dose to the treatment area and a reduction in harm caused to surrounding healthy tissue. As protons have both charge and mass, when they enter a material they lose energy by interacting with the electrons in the material via the Coulomb force. When the protons slow down, they deposit energy into the surrounding tissues. The amount of energy transferred increases as the speed of the protons decrease. Once the protons have stopped completely, all of their energy will be lost, the bulk of which is at the end of their journey, this point is known as the Bragg peak. The distance the protons travel is directly proportional to their initial energy and two protons with the same initial energy will travel the same distance in a reasonably straight line, due to their higher momenta compared to electrons[1].

In an exception to the rule described above, some of the protons will interact directly with nuclei in their path, whether within the target or the proton beam line. These interactions result in the production of various secondary radioactive particles such as gamma rays, electrons, heavy ions and neutrons. Neutrons are of particular interest as they are difficult to detect due to a lack of charge and because they have high biological effectiveness[1]. Simulating a proton therapy scenario and observing the production and behaviour of neutrons sheds a light on what would otherwise be hard to observe, particularly within the target.

2. Monte Carlo Proton Therapy Simulation

The Geant4 simulation toolkit allows one to design a detector geometry, in this case a water phantom and copper collimator mimicking a proton therapy scenario, and then begin a Run. Within the Run a number of Events, where a proton enters the geometry from just behind the collimator as if it were part of a beam[2]. As the proton moves through the geometry, its behaviour is dictated by how likely it is for an interaction to take place. The resulting behaviours, such as energy deposition or secondary particle production, from each event can therefore be normalised per source proton to compare to experimental results.

Figure 1 shows a 3D representation of the geometry used to replicate a proton therapy experiment. The target is a water phantom that is 15cm long, 17cm high and 16cm wide these dimensions are chosen to replicate a previous experiment undertaken at iThemba LABS[3]. The copper collimator has an inner radius of 50mm and an outer radius of 70mm and set is into a steel plate with an outer radius of 300mm. The collimator and plate are 80mm thick and are placed 50mm edge to edge from the water phantom.

To produce a beam, protons are created -300mm away from the world isocente within a prescribed radius of either 60 or 39mm. The protons are generated randomly within this radius so that the entire beam area will be populated.

As Geant4 can be used to model interactions at vastly different energy scales from the high energy collisions at the LHC to lower energy medical physics. The correct physics list is selected to describe the energy scale and particles being observed. Here QGSP_BIC_HP is used which models neutrons under 20MeV as well as the rest of the physics needed for this setup[4].

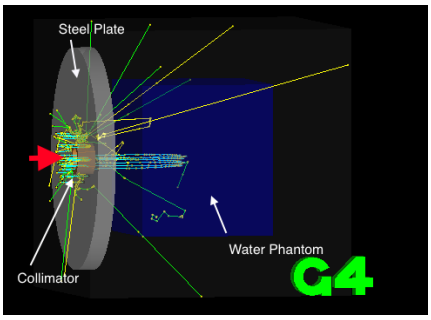

Figure 1. 3D representation of the Geant4 model, the red arrow depicts the beam direction. Tracks from 20 protons are shown in cyan, secondaries produced in the collimator and phantom are visible in other colours.

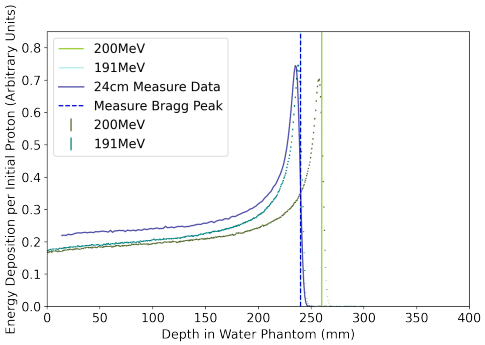

Figure 2. Figure showing the proton energy depositions of 200 and 191 MeV energy runs, compared to measured data with a 24cm Bragg peak at iThemba LABS.

3. Verification of the Model

3.1. Bragg Peak

As all results would need to be comparable to experimental data in the future, the initial energy of the protons was set to match the 24cm Bragg peak at iThemba LABS. To get the position of the Bragg peaks the following equation [5] was used with scipy.optimize.curve_fit[6]:

$$D(x) = \{\, a + \alpha e^{\frac{\tau^2\sigma^2}{2}+\tau(x-\mu)}\mathrm{Erfc}\left(\frac{x-\mu}{\sigma\sqrt{2}} + \frac{\tau\sigma}{\sqrt{2}}\right) x < \mu 0 x > \mu \tag{1}$$

Here a is a constant used to describe the near constant dose deposited before the Bragg peak. Setting $D(x) = 0$ after the Bragg peak describes the lack of dose after this point. The value μ is

the position of the peak. This equation, when fitted to the measured 24cm data, gives a Bragg peak of 24.009 ± 0.003 cm which agrees with the 24.0 ± 0.3 cm measured before. It should be noted that the uncertainties are due to the fit and not from the data, which explains why they are so small.

Initial 200 MeV protons were used, but produced a peak around 26 cm. A value of 191 MeV was found to produce a Bragg peak at 24.01 ± 0.01 cm which can be seen in Figure 2. This was chosen as the energy for all protons from this point forward[7].

3.2. Lateral Profiles

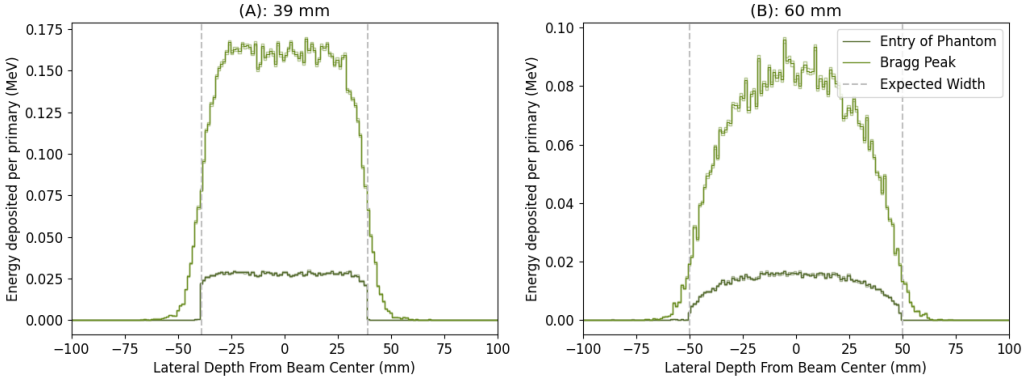

Figure 3. Lateral profiles of energy deposition by protons along the width of the water phantom at both the entry to the phantom and the Bragg Peak. (A) depicts a 39mm beam radius and (B) a 60mm beam radius.

To verify the shape of the beam, the energy deposited by protons at the entrance to the phantom and Bragg peak is examined. This is shown in Figure 3 for a beam with a radium of 39mm which passes through the copper collimator and a collimated 60mm beam. It can be seen that on entry of the phantom, the beam width is as expected. At the Bragg peak it has spread so that 6% and 2% of the proton dose is delivered outside original beam for the 39mm and 60mm beams respectively. The difference in results is because the narrower beam is not collimated and at the entry of the water phantom its profile is flat rather than dome shaped like the wider beam. As more of protons are at the beam's edge, they are more likely to exit the original beam profile when they scatter. These two beam diameters are used throughout the analysis to determine the effects of the collimator. This is done by scaling the results from the 39mm beam run per proton incident on the water phantom. This returns the internal components of the measurements as the narrower beam does not interact with the copper collimator. Internal measurements are scaled per proton incident on the phantom from the 60mm beam and subtracted to return the effects of the collimator in that run. Even though the shape of the 39mm beam is not realistic, it will not cause problems in later analysis.

4. Neutron Effects

Neutrons do not deposit their energy directly, but interact with nuclei in their path to cause cascades of secondary particles. Unlike for protons, to measure the effect of neutrons a comparison between total energy deposition in runs where neutrons and their secondaries are removed from the model and regular runs. Figure 4 shows the difference between proton energy deposition with and without neutrons to highlight how neutrons cause increased energy deposition throughout the model.

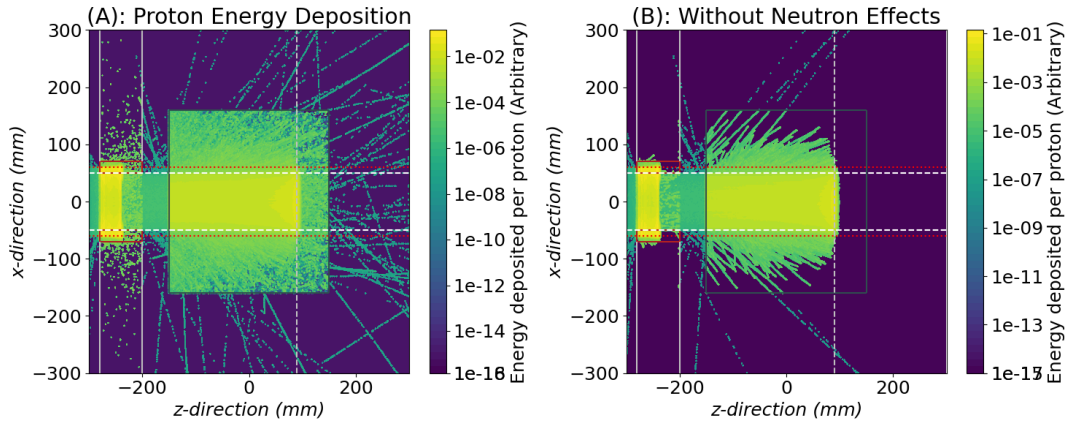

Figure 4. Plots of 2D energy deposition by protons with a 60mm beam, (A) shows the regular proton energy deposition whereas in (B) neutrons and their secondaries are removed.

The neutron populations for 39mm and 60mm proton beams are described in Figure 5 showing where neutron production takes place in the model. It can be seen in the 39mm beam that most of the neutrons are produced before the Bragg peak, where the protons' interaction cross sections with the water have maximised and the most neutrons are produced[8]. Whereas for the 60mm beam, most of the neutron production occurs within the collimator.

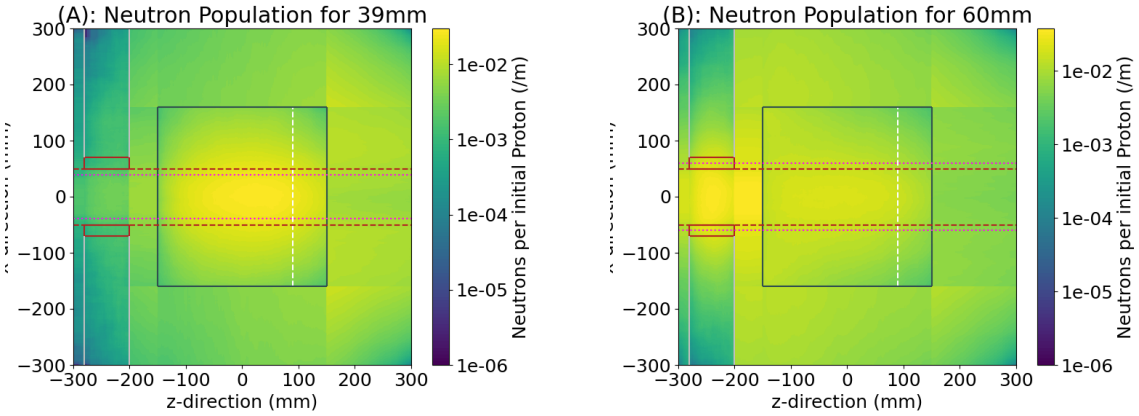

Figure 5. Plots showing the number of neutrons flowing through lines of constant x and z for a 39mm (A) and a 60mm (B) beam. The white line shows the position of the Bragg peak and the inner of the two red lines shows the width of the beam after passing through the collimator.

The 1D neutron current in the z direction is shown in Figure 6 for each of the two runs, depicting how neutrons produced in the collimator enter the water phantom. The neutron current for the 60mm beam is split into internal and external components as seen in Figure 7. The internal component is calculated by dividing the neutron current from the 39mm beam by the number of protons entering the phantom and then scaling it to the proton current from the 60mm beam. The external component is therefore the difference between the internal and the total currents. By integration, it is found that 60% of the neutron population is produced internally to the phantom.

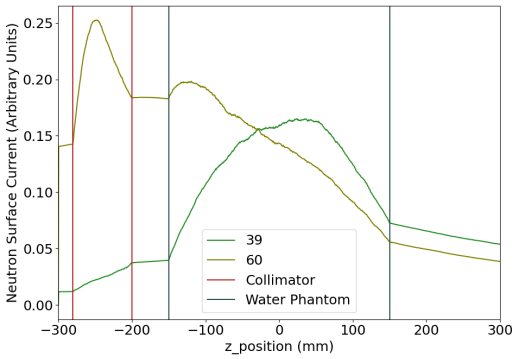

Figure 6. The neutron surface currents through the z direction for the 60mm and 39mm beams.

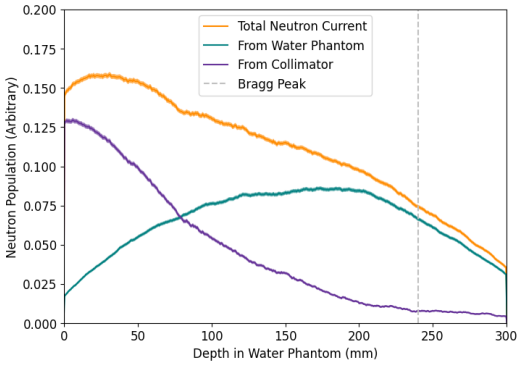

Figure 7. The neutron current from the 60mm beam split into the external and internal neutron components

5. Dosimetry Results

Dose is the standardised measure for the amount of radiation a person or object receives. The unit for absorbed dose is the Gray (Gy) given in $J.kg^1$ and it is the measure of the amount of energy deposited by ionising radiation per kilogram. The absorbed dose is obtained from the Geant4 simulation by summing the energy deposited from particles in each event in the run and dividing by the mass of the water phantom.

Table 1. Table showing different components of the total absorbed dose in the phantom as a percentage

	Dose Component (%)	**39mm**	**60mm**
A	*Therapeutic*	73.79 ± 0.03	90.14 ± 0.04
B	*Total Secondary*	26.21 ± 0.03	09.86 ± 0.04
C	*Off-Beam Proton*	23.92 ± 0.03	07.23 ± 0.04
D	*Neutron Assoc.*	00.62 ± 0.04	00.95 ± 0.06
E	*Other Secondary*	01.67 ± 0.06	01.67 ± 0.09

Table 1 shows the different components of the total absorbed dose o the phantom as a percentage. The therapeutic dose (A) is the absorbed dose delivered by protons within the beam width, this is higher for the 60mm beam as there is less lateral spread of the protons as mentioned in Section 3.2.

The total secondary dose (B), is the sum of all of the non therapeutic dose components. This is split into off-beam proton (C) which is the scattered proton dose taken from a run where neutrons and their secondaries are killed off. The neutron associated dose (D) is the difference between the secondary doses when neutrons are present in the simulation and when they are absent. Finally the other secondary dose (E) is the dose due to heavy ions, gamma rays and anything not a proton or a neutron.

Most importantly, the neutron associated dose is larger for the wider beam, due to external neutrons from the collimator, as well as there being a lower percentage of protons that make it to the phantom causing the total proton dose to decrease. The doses from the 39mm beam is then scaled per proton incident on the phantom, to get the percentage of the neutron dose produced externally for the 60mm be as: 63.8 ± 4.7 %.

6. Future Work

When designing experiments, using a simulation to shape the planning process and to benchmark expected outcomes is a valuable process. This simulation can be applied in two ways: firstly one can place smaller volumes inside the phantom and measure the dose deposited in them which can be separated into different components as done in Section 5. This can then be compared to experimental results and the results from previous simulations as done in [9].

The simulation can also be used to measure neutron fluences through areas where neutron detectors could be placed in an experimental setup as shown in Figure 8. Figures 9 and 10 show the neutron energy fluences through each possible detector placement. This sort of analysis is useful in comparing to measured neutron data, however it does not include any detector effects caused by the proton beam which would need to be accounted for.

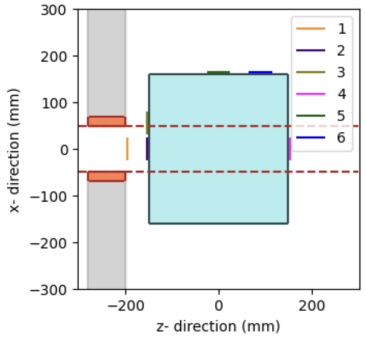

Figure 8. Schematic of possible neutron detector placements.

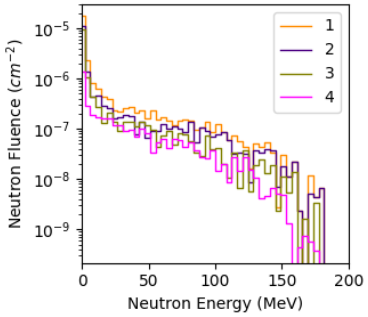

Figure 9. The neutron energy fluences through vertical planes in Figure 8

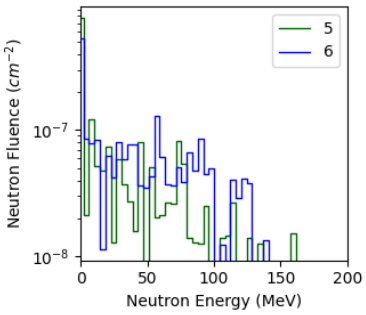

Figure 10. The neutron energy fluences through horizontal planes in Figure 8

7. Conclusion

The use of a Geant4 model in determining the effects of neutrons during proton therapy was shown. The simulation showed how the peak of neutron production is before the Bragg peak. Through comparison of the 39mm and 60mm runs it was shown the effects of the collimator on external neutron behaviour and dose. The model can be used to aid in experimental design and understanding results.

8. References

[1] Knoll G 2010 *Radiation Detection and Measurement* (Wiley) ISBN 9780470131480

[2] Unknown 2003 Basic structure of basic structure of the geant4 simulation toolkit the geant4 simulation toolkit URL `https://www.ge.infn.it/geant4/training/portland/basicStructure.pdf`

[3] Personal Communications with Charlot van der Voorde at iThemba LABS

[4] Unknown Reference physics lists URL `https://geant4.web.cern.ch/node/155`

[5] Lambrechts K 2015 Fitting the bragg peak for accurate proton range determination URL `https://fse.studenttheses.ub.rug.nl/13103/1/eindversie_bacheloronderzoek`$_{K1}$*.pdf*

[6] Community T S 2022 scipy.optimize.curve_fit documentation URL `https://docs.scipy.org/doc/scipy/reference/generated/scipy.optimize.curve`$_f$*it.html*

[7] Jeyasugiththan J 2021 Measuring prompt gamma-ray emissions from elements found in tissue during passive-beam proton therapy

[8] Jia S B, Hadizadeh M H, Mowlavi A A and Loushab M E 2014 *Reports of Practical Oncology And Radiotherapy* **19** 376–384 ISSN 1507-1367

[9] van Deventer S 2021 Investigation of secondary neutron production during proton therapy